

## 1 Supplemental Material

### 2 S1. Study Area



3  
4 **Figure S1.** Photo of Bakersfield and the South San Joaquin Valley from the NASA (Earth  
5 Research ER-2 airplane at 20-km altitude. Blue-white arrows show approximate direction of  
6 prevailing winds, oil fields near Bakersfield labeled. Photo courtesy Stuart Broce, Pilot, NASA  
7 Armstrong Flight Research Center.

8

### 9 S2. Platforms

#### 10 S2.1. Surface – AMOG Surveyor

11 Mobile surface *in situ* measurements using Cavity RingDown Spectroscopy (CRDS) (Pétron et  
12 al., 2012; Farrell et al., 2013) and open path spectroscopy (Sun et al., 2014) are becoming more  
13 common. Surface data were collected for the *GOSAT COMEX Experiment* by the AMOG  
14 (AutoMOBILE trace Gas) Surveyor (Leifer et al., 2014). AMOG Surveyor is a commuter car  
15 (Versa SP, Nissan, Japan) that is modified for mobile high-speed, high-spatial resolution  
16 observations of meteorology (winds, temperature, and pressure), gases (greenhouse and other  
17 trace), and remote sensing parameters (Fig. S2).



18

19

20 **Figure S2.** (a) AMOG Surveyor in the Transverse Coastal Range (1300 m) – San Joaquin Valley  
 21 in background. (b) Cockpit view of gauges, security video, rear video, real-time data display.  $V_A$ ,  
 22  $V_{FB}$ ,  $V_{RB}$ ,  $V_I$  – voltages for alternator, front battery, rear battery, inverter.  $T_I$ ,  $T_O$ ,  $T_W$  – temperatures  
 23 for inverter, engine oil, and radiator water.  $P_T$ ,  $P_O$ ,  $P_W$ ,  $P_S$ ,  $P_C$ ,  $P_R$  – pressures for tires, oil, water  
 24 suspension, compressor, and regulated air for chemical scrubbers. (c) AMOG Surveyor in Sierra  
 25 Nevada Mountains, roof package labeled.

26

27 Analyzers: AMOG Surveyor draws air down two ½” PFA Teflon sample lines from 5 and 3 m  
 28 above ground into a configurable range of gas analyzers by a high flow (850 lpm, 30 cfm)  
 29 vacuum pump (Edwards, GVSP30). The higher sample line connects to several analyzers  
 30 including a Fast-flow, enhanced performance Greenhouse Gas Analyzer (FGGA, [enhanced](#)  
 31 [model, Los Gatos Research, CA](#)), which uses Integrated Cavity Off-Axis Spectrometer-Cavity  
 32 Enhanced Absorption Spectroscopy (ICOAS-CEAS) and measures carbon dioxide, CO<sub>2</sub>,  
 33 methane, CH<sub>4</sub>, and water vapor, H<sub>2</sub>O, at up to 10 Hz (Model 911-0010, Los Gatos Research, Inc.,  
 34 Mountain View, CA). AMOG also measures carbonyl sulfide (COS) and carbon monoxide (CO)  
 35 with an ICOAS-CRDS analyzer (Model 907-0028, Los Gatos Research, Inc., Mountain View,

36 CA). An additional sample line collects feeds an ICOAS-CRDS that measure ammonia (NH<sub>3</sub>)  
37 and hydrogen sulfide (H<sub>2</sub>S). For all CEAS analyzers, dry values are used. Also, three  
38 chemiluminescence trace gas analyzers measure nitric oxide (NO) and nitrogen oxides (NO<sub>x</sub>) at  
39 0.1 Hz at 25 ppt accuracy (42TL, ThermoFischer Scientific, Waltham, MA), and ozone (O<sub>3</sub>) at  
40 0.25 Hz at 1 ppb accuracy (42C, ThermoFischer Scientific, Waltham, MA), and sulfur dioxide  
41 (SO<sub>2</sub>) at 0.1 Hz at 1 ppb accuracy (450C, ThermoFischer Scientific, Waltham, MA). This

42 accuracy is from the manufacturer and is based on 24 hour drift. Better accuracy is achieved by  
43 hourly zero gas measurements using chemically sparged air (Type CI, Cameron Great Lakes,  
44 OH), which in the laboratory improved accuracy to 50 ppt. Given that SO<sub>2</sub> and H<sub>2</sub>S atmospheric  
45 concentrations are typically less than 1 ppb in California, this was an important improvement.

46  
47 The FGGA is calibrated with an air calibration standard for greenhouse gases (CH<sub>4</sub>: 1.981 ppmv;  
48 CO<sub>2</sub>: 404 ppmv; balance ultrapure air) and are stable to 1 ppb for CH<sub>4</sub> over 24 hours, and 0.12  
49 ppm for CO<sub>2</sub> over 24 hours. Accuracy is <0.03%. Calibrations are performed before and after  
50 each field collect. The 49i was cross-calibrated with the AJAX O<sub>3</sub> analyzer to 1 ppb, and during  
51 a repeat cross calibration several months later had maintained its calibration to between 1 and 2  
52 ppb.

53  
54  
55 Meteorology: A sonic anemometer (VMT700, Vaisala, Finland) is mounted 1.4 m above the roof  
56 and measures two-dimensional winds. Estimated accuracy is approximately 10° and 0.3 m s<sup>-1</sup> for  
57 wind speeds above 1.5 m s<sup>-1</sup>; however, accuracy improves with vehicle velocity and wind speed  
58 as vehicle flow stream line interferences are reduced. Accuracy was determined empirically by  
59 driving several kilometers back and forth on a rural road in an open area in the early morning and  
60 comparing measured winds in the two directions. Note, these accuracies are greater than the  
61 manufacturer maximum error. At lower wind speeds, accuracy appears to be closer to 0.2 m s<sup>-1</sup>,  
62 and 15-20°; however, is extremely challenging to determine. Still, filtering, nocturnal wind data  
63 generally agrees well (~10°) with expectations from topographic forcing at wind speeds of ~0.2 -  
64 0.5 m s<sup>-1</sup> on large spatial scales (tens of kilometers) for highway speed (140 km hr<sup>-1</sup>) data. In  
65 general, winds are more accurate than stated if the winds are from within 30° of forward  
66 direction, as stated if they are from the side, unless strong (>~4 m s<sup>-1</sup>), in which case they are

ira leifer 12/13/17 9:35 AM

Moved (insertion) [1]

ira leifer 12/13/17 9:34 AM

Deleted: .

ira leifer 12/13/17 9:38 AM

Deleted: The

ira leifer 12/13/17 9:38 AM

Deleted: 450C can achieve 50 ppt accuracy by

ira leifer 12/13/17 9:39 AM

Deleted: PA

ira leifer 12/13/17 9:39 AM

Formatted: Highlight

ira leifer 12/13/17 9:38 AM

Deleted: .

ira leifer 12/13/17 9:42 AM

Formatted: Subscript

ira leifer 12/13/17 9:42 AM

Formatted: Subscript

ira leifer 12/13/17 9:34 AM

Deleted: .

ira leifer 12/13/17 9:35 AM

Moved up [1]: The 450C can achieve 50 ppt accuracy by hourly zero gas measurements using chemically sparged air (Type CI, Cameron Great Lakes, PA).

ira leifer 12/13/17 9:47 AM

Formatted: Subscript

ira leifer 12/13/17 10:01 AM

Deleted: Recent

ira leifer 12/13/17 10:03 AM

Formatted: Superscript

79 equally accurate and very poor if from within ~15° of the behind direction. As a result, tail winds  
80 are not evaluated.

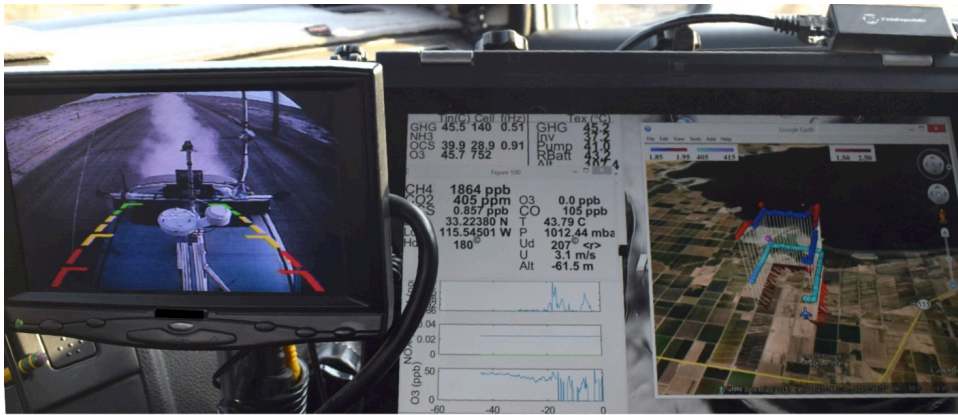
81  
82 AMOG system improvements beyond (2014) include a high speed thermocouple (50416-T,  
83 Cooper-Atkins, CT) and a high accuracy (0.2 hPa) pressure sensor (61320V RM Young Co.,  
84 MI), connected by a stainless steel line into a roof passive radiation shield (7710, Davis  
85 Instruments, CA) to reduce dynamic pressure effects. The radiation shield also includes a Type T  
86 thermocouple (Omega, CT) digitized at 0.03°C resolution (CB-7018, Measurement Computing,  
87 MA). A solar insolation sensor is digitized at 16 bit and 1 Hz (CB-7017, Measurement  
88 Computing, MA). Two (redundant) Global Navigation Satellite Systems (19X HVS, Garmin,  
89 KS) that use the GLONASS, GPS, Galileo, and QZSS satellites provide position information at  
90 10 Hz.

91  
92 Vehicle Power: To support the science package (~1.8 kW), with clean DC and AC power,  
93 AMOG has a 3.3 kW alternator (Nations Alternator, Cape Girardeau, MO), with a 2.7 kW  
94 inverter (2810M, Outback Power, Arlington, OR), and a dual voltage conversion 2.4kW  
95 uninterruptible power supply (Tripp Lite SU3000RTXL3U) backed by three, deep cycle gel  
96 batteries for a total of 250 Amp-hours (Lifeline Batteries, WI; 6FM100H, Vision, MO; PVX-  
97 1040T, Sun Xtender, CA) with active isolation (Dual Rectifier Isolator, Stolper International,  
98 Inc., San Diego, CA). The 100 A-hr batteries and inverter are mounted in the cabin floor center  
99 to improve stability. The DC system includes a 1-farad capacitor to stabilize against surges.

100  
101 AMOG Surveyor weighs ~1 ton above stock, with significant safety implications, which were  
102 addressed by enhancements to handling, suspension, and braking. Specifically, front drilled and  
103 slotted ceramic brakes (F2473, Black Hart). Suspension modifications include rear airbag  
104 suspension (NV-NINV-RBK, X2 Industries, AZ), adjustable rear truck shocks (for a Ford F-  
105 150), performance coil-over front struts (TSC123, Tanabe, Japan), strut tower bar, sway bar, and  
106 ladder brace.

ira leifer 12/13/17 10:03 AM

Deleted: science



108  
 109 **Figure S3.** AMOG Surveyor cockpit view showing real-time display (right) and rear camera  
 110 view in the Salton Sea, CA. Methane ( $\text{CH}_4$ ), carbon dioxide ( $\text{CO}_2$ ), and wind speed ( $U$ ) and  
 111 direction ( $U_d$ ) are shown in the Google Earth visualization window. Rolling display (lower left)  
 112 shows  $\text{CH}_4$ , nitrogen oxides ( $\text{NO}_x$ ) and ozone ( $\text{O}_3$ ). Diagnostics window (upper left) shows cell  
 113 pressures and temperatures and key temperatures.

114  
 115 Data Handling and Integration: A touchscreen tablet (SpectreX360, HP) logs data  
 116 asynchronously from instruments and sensors through several serial Ethernet servers (5450  
 117 NPort, Moxa, Brea, CA) and industrial switches (EDS205, Moxa, Brea, CA). Logged data are  
 118 mirrored to a SSD LAN drive in AMOG. Acquisition time is identified to  $\sim 30$  milliseconds from  
 119 the position of the data in the serial server buffer queues.

120  
 121 Custom software integrates the data streams and creates real time visualizations of multiple  
 122 parameters in the Google Earth environment to enable adaptive surveying (Thompson et al.,  
 123 2015). In adaptive surveying, the survey route is modified based on real time environmental  
 124 conditions (winds, new/unexpected sources, etc.). GoogleEarth visualizations are displayed on  
 125 one to several computers in AMOG Surveyor (**Fig. S3**) and remotely through cloud mirroring.  
 126 Viewing algorithms automatically follow the vehicle, rotated to display wind vectors, and adjust  
 127 the view altitude based on vehicle velocity. Algorithms minimize track overlap confusion  
 128 through selective use of transparency, i.e., when AMOG Surveyor returns on the same course, or  
 129 loops around. Rolling history displays of gas concentrations are useful for identifying recently



130 transected plumes. Other windows display AMOG Surveyor and analyzer diagnostics, and real  
131 time analyzer gas and meteorology values.

132

### 133 **S2.2. Airborne - AJAX**

134 Airborne *in situ* data were collected by AJAX (Alpha Jet Atmospheric eXperiment), operated  
135 from NASA Ames Research Center (ARC) at Moffett Field, CA. The alpha jet aircraft, which  
136 has been modified for science missions, measures carbon dioxide and methane (Picarro Inc.,  
137 model G2301-m), ozone ([Model 205](#), 2B Technologies Inc.), formaldehyde (Compact  
138 Formaldehyde Fluorescence Experiment, COFFEE), and meteorological parameters including  
139 3D winds by the Meteorological Measurement System (MMS), a NASA developed system  
140 [\(<https://earthscience.arc.nasa.gov/mms>\)](https://earthscience.arc.nasa.gov/mms), from two externally-mounted wing pods (**Fig. S4**). MMS  
141 accracies are  $\pm 1 \text{ m s}^{-1}$  horizontal,  $0.3 \text{ m s}^{-1}$  vertical. The greenhouse instrument was calibrated  
142 using whole-air (National Oceanic and Atmospheric Administration) standards before and after  
143 aircraft deployment. The ozone sensor is frequently calibrated to a NIST- traceable standard.  
144 Further details on the aircraft and instrumentation are reported by Hamill et al. (2015); Tanaka et  
145 al. (2016) and Yates et al. (2013).

146



147  
148 **Figure S4.** AJAX photo. Courtesy Warren Gore, NASA Ames Research Center.

149

ira leifer 12/13/17 9:33 AM  
**Deleted:** ,

ira leifer 12/13/17 10:30 AM  
**Deleted:** {MMS, 2017 #2712;MMS, 2017 #2712}model 205

ira leifer 12/13/17 10:31 AM  
**Deleted:** (

ira leifer 12/13/17 10:31 AM  
**Deleted:** ,

ira leifer 12/13/17 10:33 AM  
**Formatted:** Font:11 pt

ira leifer 12/13/17 10:33 AM  
**Formatted:** Font:Times, 11 pt

ira leifer 12/13/17 10:31 AM  
**Deleted:** {MMS, 2017 #2712} MMS)

ira leifer 12/13/17 10:35 AM  
**Formatted:** Superscript

ira leifer 12/13/17 10:35 AM  
**Formatted:** Superscript

156 The Alpha Jet is owned by H211, LLC, a collaborative partner with NASA. It is a tactical strike  
157 fighter developed by Dassault-Breguet and Dornier through a German-French NATO  
158 collaboration. Dassault concurrently developed a trainer version of the Alpha Jet that is still in  
159 service with the French Air Force. Carrying a crew of two, it has a length of 12.2 m, a wingspan  
160 of 9.2 m, and a height of 4.2 m. Its empty weight is 3540 kg and a maximum takeoff weight of  
161 8000 kg. It has a ceiling of 15,545 m, speed of 280 – 930 km/hr, and a range of approximately  
162 1930 km with full fuel.

163

164 The Alpha Jet stationed at NASA Ames – Moffett Field is operated in accordance with an FAA  
165 Experimental Certificate of Airworthiness. It has a 2 to 2.5 hr flight duration, permitting up to  
166 two missions per day with appropriate crew changes. Three highly experienced H211 pilots are  
167 FAA Type Certificated to fly the Alpha Jet, and science test flights began in September 2010.  
168 Following a complete avionics update and installation of the NASA-specified payload  
169 management and control system in early 2009, the Alpha has proven extremely robust and  
170 reliable. Its fleet safety record as a twin-engine, all weather jet is excellent, and its modern  
171 Snecma engines produce a noise signature equivalent to current generation Stage III noise  
172 compliant turbofan aircraft.

173

174 H211 has provided significant upgrades to the aircraft to support scientific studies. Extensive  
175 wiring and cabling provisions have been installed to both wing pod locations, as well as the  
176 centerline pod, to allow for distribution of 120 and 26 volt AC and 28 volt DC to each wing pod,  
177 as well as additional 120 volt AC and 28 volt DC service to the centerline pod. Redundant  
178 heavy-duty Ethernet cables have been provided from the wing pods to the centerline pod and  
179 backseat control console. An operator interface panel has been installed in the rear cockpit to  
180 allow power on/off/failure interface to each scientific instrument. Additionally, the pilot has a  
181 payload master power switch that can remove all electrical power from the NASA payloads in  
182 the event an abnormal electrical condition is encountered.

183

184 Multiple redundant Garmin G600/G530/G430/G696 systems record and display position,  
185 attitude, heading, altitude, true airspeed, groundspeed, true air temperature, wind speed, wind  
186 direction, and a wide variety of additional data through dual digital air data computers. This

ira leifer 12/13/17 11:36 AM

Deleted: -

188 information is recorded for science use. A digital autopilot system allows highly accurate  
189 heading and track control via GPS steering, plus precise altitude control during air sampling  
190 missions. AJAX flights can also be followed in real-time using the NASA Airborne Science  
191 Mission Tool Suite.

192

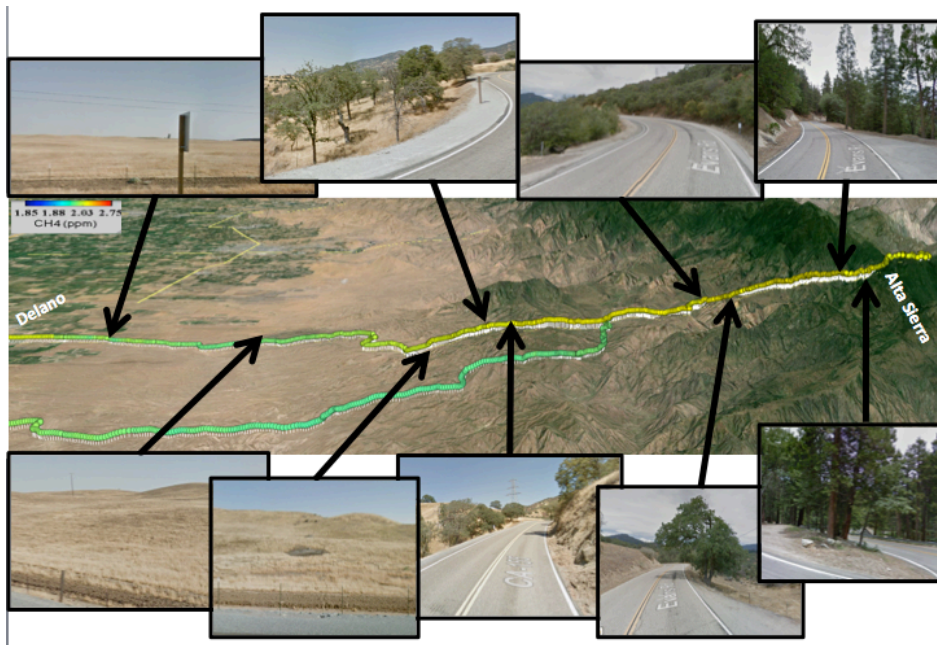
193 Two wing-mounted pods have been modified by NASA-ARC to carry instrumentation, with  
194 three down-looking window ports available on each pod. Each wing pod has an approximate  
195 available volume of 0.1 cubic meter, with a maximum payload weight of 136 kg. The centerline  
196 pod has two payload areas of approximately 86.4 x 25.4 x 30.5 cm and 68.6 x 16.5 x 25.4 cm,  
197 carrying combined payloads up to 136 kg total.

198

#### 199 **S4. Upwind Profile**

200 An upwind pre-survey east-west transect was conducted by AMOG from Delano (~70 m) on the  
201 floor of the San Joaquin Valley to Alta Sierra (~1750 m) on the ridge of the Greenhorn  
202 Mountains in the Sierra Nevada Mountain Range (Fig. S5). This survey passed through a range  
203 of surface topography and vegetation and canopy types. Example Google Maps “street images”  
204 show variation from flat grasslands to rolling grass covered hills, to scattered low oak trees, to at  
205 the highest altitudes, dense, tall pine forests. The road shifts from an initial gradual rise while  
206 following a primarily straight and gently curved pathway, to steeper climbs cut into steep slopes  
207 with sharp curves, and even hairpin curves.





208  
 209 **Figure S5** – Sierra Nevada Mountain Range vertical profile, and Google maps street images  
 210 showing changing terrain. [Data key on figure.](#)

211

212 **S5. Derivation of the background data curtain**

213 The background data plane was calculated from the probability distributions on the left and on  
 214 the right side of the transects at each altitude. Then, the CH<sub>4</sub> for the peak of each distribution is  
 215 assigned to the left and right side of each altitude transect and linearly interpolated. Finally, the  
 216 distribution is vertically interpolated to fill in the background data plane (Fig. S6).

217

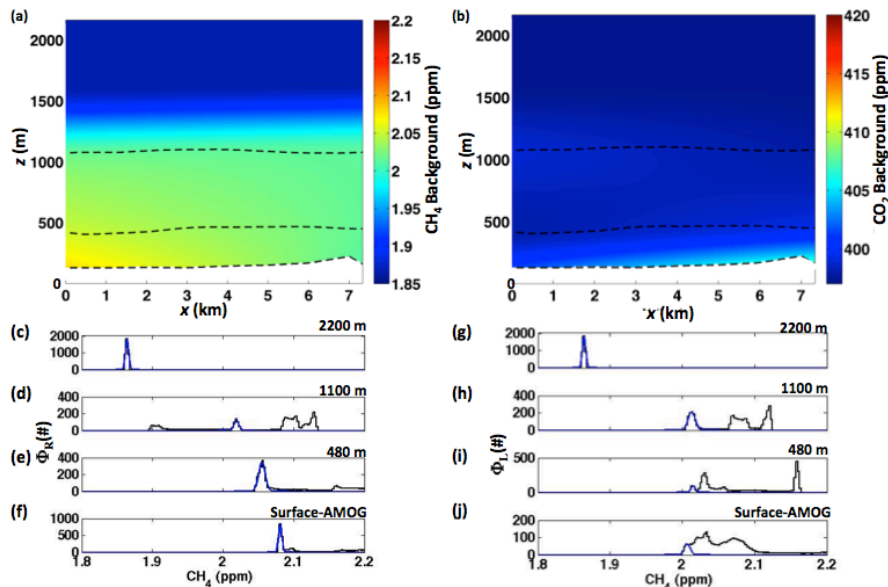
218 The background data plane (Fig. S6) for transect  $\gamma-\gamma'$  (Fig. 7) showed a trend of increasing CH<sub>4</sub>  
 219 towards the west, rising more than ~25 ppb, at both the surface and at 480 m altitude. In contrast,  
 220 background CO<sub>2</sub> across the data curtain was quite uniform.

221

222 Anomaly concentration was relative to the background concentration curtain (Fig. S6a & 6b) and  
 223 was derived by estimating the background concentration at each transect altitude from fitting a

- ira leifer 12/13/17 8:58 PM  
Formatted: Font:12 pt
- ira leifer 12/13/17 8:58 PM  
Formatted: Font:12 pt, Subscript
- ira leifer 12/13/17 8:58 PM  
Formatted: Font:12 pt
- ira leifer 12/13/17 8:58 PM  
Formatted: Font:12 pt
- ira leifer 12/13/17 8:58 PM  
Formatted: Font:12 pt

224 Gaussian to the background occurrence concentration distribution and using the distribution peak  
225 as the background concentration (Fig. S6c-S6f). The methodology is described in Sect. 2.4.



226  
227 **Figure S6** – Background (a) methane ( $\text{CH}_4$ ) and (b) carbon dioxide ( $\text{CO}_2$ ) data curtain with  
228 respect to lateral east distance ( $x$ ) relative to  $119.0023^\circ\text{W}$ ,  $35.3842^\circ\text{N}$  for data plane  $\gamma\text{-}\gamma'$  and  
229 altitude ( $z$ ). Dashed line shows data altitudes. (c-f)  $\text{CH}_4$  left side probability distribution and (g-j)  
230  $\text{CH}_4$  right side probability distributions ( $\Phi$ ).

231

ira leifer 12/12/17 8:02 PM

Deleted: 5

ira leifer 12/13/17 11:38 AM

Deleted: .

ira leifer 12/13/17 11:38 AM

Formatted: Font:Italic

ira leifer 12/13/17 8:51 PM

Formatted: Not Superscript/ Subscript

ira leifer 12/13/17 8:52 PM

Deleted:  $\text{CO}_2$

ira leifer 12/13/17 8:52 PM

Deleted: .

ira leifer 12/13/17 8:52 PM

Deleted: data

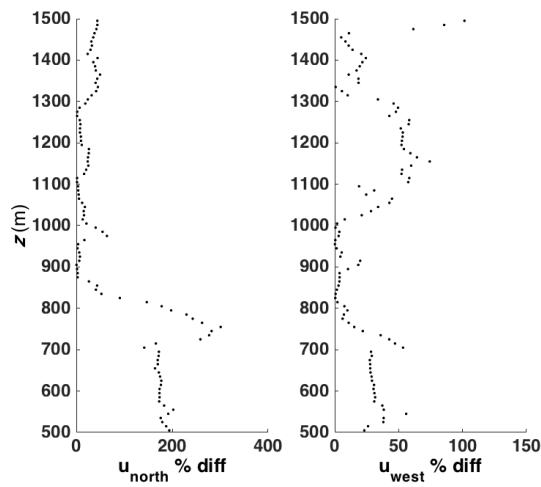


Figure S7 – Comparison between AMOG (a)  $u_{north}$ , (b) and  $u_{west}$ .

ira leifer 12/13/17 9:14 PM

Formatted: Figure

ira leifer 12/13/17 9:15 PM

Formatted: Font:Italic

ira leifer 12/13/17 9:15 PM

Formatted: Font:Italic, Subscript

237

238

239

240

## 241 References

- 242 Farrell, P., Leifer, I., Culling, D., 2013. Transcontinental methane measurements: Part 1. A  
 243 mobile surface platform for source investigations. *Atmospheric Environment* 74, 422-431,  
 244 doi:10.1016/j.atmosenv.2013.02.014
- 245 Hamill, P., Iraci, L.T., Yates, E.L., Gore, W., Bui, T.P., Tanaka, T., Loewenstein, M., 2015. A  
 246 new instrumented airborne platform for atmospheric research. *Bulletin of the American  
 247 Meteorological Society* 97, doi:10.1175/BAMS-D-14-00241.1
- 248 Leifer, I., Melton, C., Manish, G., Leen, B., 2014. Mobile monitoring of methane leakage. *Gases  
 249 and Instrumentation* July/August 2014, 20-24,
- 250 Pétron, G., Frost, G., Miller, B.R., Hirsch, A.I., Montzka, S.A., Karion, A., Trainer, M.,  
 251 Sweeney, C., Andrews, A.E., Miller, L., Kofler, J., Bar-Ilan, A., Dlugokencky, E.J., Patrick,  
 252 L., Moore, C.T.J., Ryerson, T.B., Siso, C., Kolodzey, W., Lang, P.M., Conway, T., Novelli,  
 253 P., Masarie, K., Hall, B., Guenther, D., Kitzis, D., Miller, J., Welsh, D., Wolfe, D., Neff, W.,  
 254 Tans, P., 2012. Hydrocarbon emissions characterization in the Colorado Front Range: A pilot  
 255 study. *J. Geophys. Res.* 117, D04304, doi:10.1029/2011jd016360
- 256 Sun, K., Tao, L., Miller, D.J., Khan, A.M., Zondlo, M.A., 2014. On-road ammonia emissions  
 257 characterized by mobile, open-path measurements. *Environmental Science & Technology* 48,  
 258 3943-3950, doi:10.1021/es4047704
- 259 Tanaka, T., Yates, E., Iraci, L.T., Johnson, M.S., Gore, W., Tadi, J.M., Loewenstein, M., Kuze,  
 260 A., Frankenberg, C., Butz, A., Yoshida, Y., 2016. Two-year comparison of airborne  
 261 measurements of CO<sub>2</sub> and CH<sub>4</sub> with GOSAT at Railroad Valley,

262 Nevada. IEEE Transactions on Geoscience and Remote Sensing 54, 4367-4375,  
263 doi:10.1109/TGRS.2016.2539973  
264 Thompson, D., Leifer, I., Bovensman, H., Eastwood, M., Fladeland, M., Frankenberg, C.,  
265 Gerilowski, K., Green, R., Krautwurst, S., Krings, T., Luna, B., Thorpe, A.K., 2015. Real-  
266 time remote detection and measurement for airborne imaging spectroscopy: A case study  
267 with methane. Atmospheric Measurement Techniques 8, 1-46, doi:10.5194/amtd-8-1-2015  
268 Yates, E.L., Iraci, L.T., Roby, M.C., Pierce, R.B., Johnson, M.S., Reddy, P.J., Tadić, J.M.,  
269 Loewenstein, M., Gore, W., 2013. Airborne observations and modeling of springtime  
270 stratosphere-to-troposphere transport over California. Atmos. Chem. Phys. 13, 12481-12494,  
271 doi:10.5194/acp-13-12481-2013  
272